JOURNAL OF SPACECRAFT AND ROCKETS
Vol. 43, No. 5, September–October 2006

Computer Simulation and its Experimental Verification of Atomic Oxygen Concentration

Masahito Tagawa,* Koshi Matsumoto,† Hiroaki Doi,‡ and Kumiko Yokota§
Kobe University, Kobe 657-8501, Japan

DOI: 10.2514/1.15037

Feasibility of atomic oxygen concentration in low Earth orbit space environment for material testing was studied. To maximize the concentration efficiency, trajectories of the atomic oxygen reflected at the reflector surface were computer-simulated based on the Hard-Cube model, which can deal with inelastic scattering events at the solid surface. The difference in incident and exit angles was predicted to be at most 5 deg depending on the incident angle. The computational results were compared with the experimental results using a 5 eV hyperthermal atomic oxygen beam. A good correlation between the numerical and experimental results was identified. It was experimentally demonstrated that the atomic oxygen flux could be increased six times greater than its original value with three reflective mirrors.

Nomenclature

A	=	electrode area of quartz crystal microbalance
E_i	=	incident energy
f_0	=	resonant frequency
k	=	Boltzmann constant
m_g	=	mass of incident atom
m_s	=	mass of surface moiety
N	=	frequency constant
T	=	surface temperature
θ_r	=	exit angle
θ_i	=	incident angle
ρ	=	density of quartz
ΔW	=	mass change of quartz crystal microbalance
Δf	=	frequency shift of quartz crystal microbalance
μ	=	ratio of the mass of incident atom and surface moiety, m_g/m_s

I. Introduction

ONE of the problems in material testing in flight experiments is a low degree of freedom-of-exposure conditions. For example, because atomic oxygen (AO) flux in a flight experiment is constant, a multiple fluence exposure testing can only be achieved by changing exposure time. If AO flux at a sample surface in low Earth orbit (LEO) can be adjusted, it may reduce cost and time for a material testing in LEO and provide wider knowledge of materials' response in space environment. Moreover, an acceleration test capability in LEO would be realized, if AO flux can be increased in LEO. Such an acceleration test capability would be valuable to verify the survivability of materials in space environment especially for AO-resistant materials that require greater AO fluences to examine the effect of atomic oxygen exposure. Moreover, high-AO flux reduces exposure time in LEO and may eliminate contamination problems in material tests. Therefore, use of high-efficiency AO concentrators will be useful to increase the degree of freedom in material tests conducted in LEO. However, AO in LEO is a noncharged species such that any electromagnetic optics, which are widely applied to focus ions and electrons, cannot be applied to focus AO. The only practical method to change trajectories of noncharged particles is using reflective solid surfaces. Such an AO-focusing device has already been evaluated by STS-85 in 1997 (see Sec. II for detail). Three parabolic horns with three different sizes have been tested to collect AO for acceleration testing of materials. However, it has been reported that the concentration factors were lower than the expectation [1].

In this paper, an attempt to develop a high-efficiency AO concentration device is reported. Basic properties of AO reflection at the solid surface were investigated to develop AO concentrators. Some key points to achieve high-efficiency in atomic oxygen concentration will be addressed based on the computational results. The computational results were experimentally verified with the hyperthermal AO beam facility at Kobe University [2–4].

II. Atomic Oxygen Focusing Device Aboard STS-85

The specimens in concentrators, which were conceived to increase the AO flux on the specimens by aluminum parabolic horns, have been flown as a part of the Effects of Space Environment on Materials Experiment (ESEM) program, which was onboard STS-85 [1]. The AO concentrators were expected to have x4, x9, and x16 accelerations (see Fig. 1). STS-85 was launched at 1041 hrs EDT on 7 August 1997. The ESEM pallet faced the ram direction for a total of 77.00 h, 52.48 h while at an altitude of 287–296 km, and 24.52 h while at an altitude of 256 km. The orbiter touched down at 0708 hrs EDT on 19 August 1997. AO fluence was estimated from the mass change of Kapton witness sample. By assuming the erosion rate of Kapton to be 3.0×10^{-24} $\mathrm{cm}^3/\mathrm{atom}$, AO fluence during the flight was estimated to be 8.6×10^{19} $\mathrm{atoms/cm}^2$. In contrast, a detailed computer model predicted the total fluence of AO during the mission to be 1.0×10^{20} $\mathrm{atoms/cm}^2$.

After retrieval, a laser profilometry was used to measure the recession of specimens flown in the AO concentrators. Table 1 is a summary of the data for the average thickness changes of Kapton specimens placed under the focusing concentrators during the ESEM experiment flight. From the mass loss data of the Kapton witness sample, the recession of 2.6μm is expected on the x1 Kapton specimen. As is shown in Table 1, the reaction rates are increased over ambient rates, but the erosion depths do not correlate with acceleration factors at x9 and x16. It was estimated that the pressure buildup in each focusing concentrator provides an opportunity for

---

Received 26 September 2005; revision received 15 January 2006; accepted for publication 21 January 2006.

*Associate Professor, Department of Mechanical Engineering, Rokko-dai 1-1, Nada, Kobe 657-8501; tagawa@mech.kobe-u.ac.jp. Member AIAA, Corresponding author.

†Student, Graduate School of Natural Science, Rokko-dai 1-1, Nada, Kobe 657-8501.

‡Student, Department of Mechanical Engineering, Rokko-dai 1-1, Nada, Kobe 657-8501.

§Research Staff, Department of Mechanical Engineering, Rokko-dai 1-1, Nada, Kobe 657-8501.

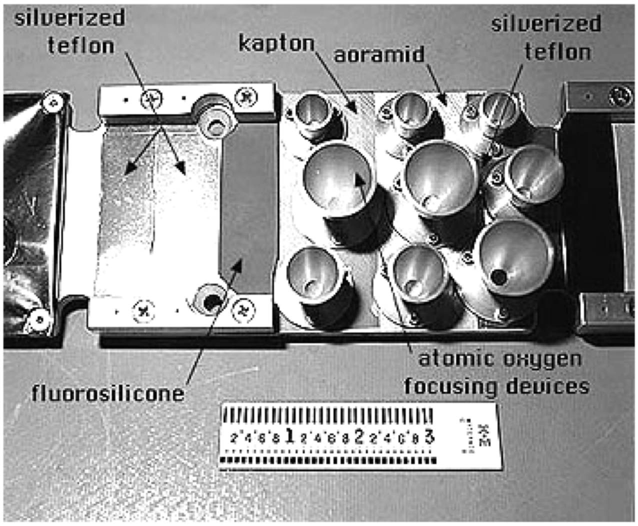

Fig. 1 AO-focusing devices flown in ESEM experiment aboard STS-85 [1].

Table 1 Recession of the polyimide films exposed to AO under focusing devices flown in ESEM experiment aboard STS-85 [1]

Acceleration factors				
Focusing devices	×1	×4	×9	×16
Erosion depth of Kapton, μm	2.6	9	18	15

recombination of AO to O_2 molecule which reduces the reactivity of AO.

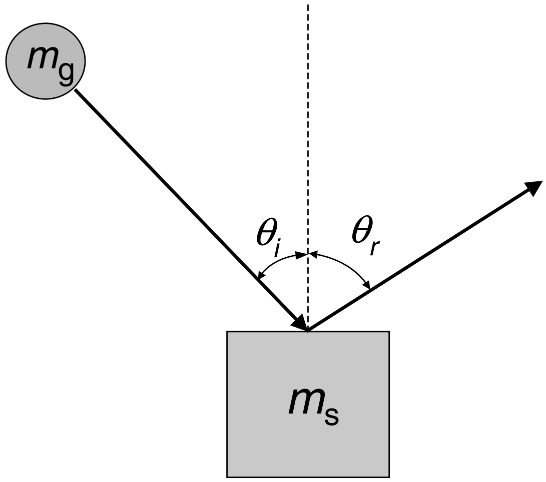

Fig. 2 Principle of the Hard-Cube model.

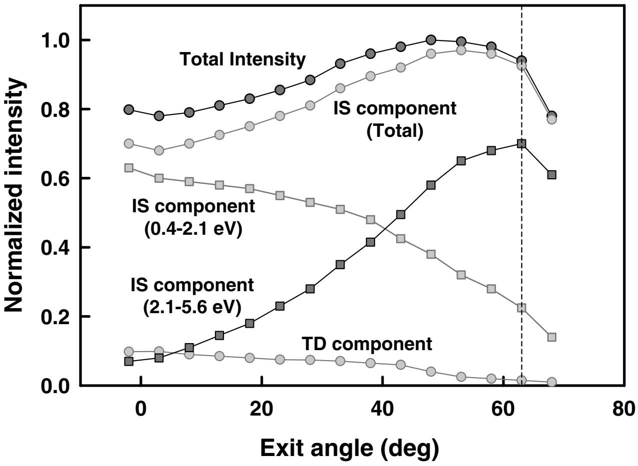

Fig. 3 F atom scattering data reported by Minton et al. [6].

III. Computer Simulation Based on Hard-Cube Model

Unlike light scattering, atoms and molecules lose their translational energies in the scattering event at the reflector surface and usually do not exit in the specular direction. To maximize the concentration efficiency of AO, the prediction of average exit angle of the reflected AO is essential. For this purpose, computer simulation of the scattering event of AO at the reflector surface was performed using the Hard-Cube model [5]. The Hard-Cube model is one of the primitive methods to simulate a scattering event at solid surface. It assumes elastic collision of hard-atom (ball) and hard-surface moiety (cube) that vibrates in the direction of surface normal. The principle of the Hard-Cube model is shown in Fig. 2. In this model, the following assumptions are used: 1) gas atoms and solid surface collide instantaneously and elastically, 2) collisions do not affect the tangential component of the velocity of the gas atoms, 3) cubes independently move each other, 4) a gas atom leaves the solid surface after a single collision, and 5) cubes thermally vibrate only in the direction of surface normal. The model is able to predict the average scattering angle of the scattered gas atoms. The average exit angle θ_r of AO is expressed in the following formula:

$$\theta_r = \cot^{-1}\left[\left(\frac{1-\mu}{1+\mu} + \frac{\mu}{1+\mu}\frac{kT}{E_i}\frac{1}{\cos^2\theta_i}\right)\cot\theta_i\right] \tag{1}$$

where θ_i is the incident angle, E_i is the incident energy, k is the Boltzmann constant, T is the surface temperature, and μ is the ratio of the mass of incident atom and surface moiety m_g/m_s. The only unknown variable in Fig. 2 is the effective surface mass m_s. In this study, m_s was determined by the comparison with the experimental data of hyperthermal F atom scattering at Si (001) surface reported by Minton et al. [6]. In the time-of-flight (TOF) spectra of the scattered atom, two components are often obvious, i.e., thermal desorption (TD) and inelastic (IS) components. Minton et al. divided IS components into two energy ranges, i.e., low-energy (0.4–2.1 eV) and high-energy (2.1–5.6 eV) components. Figure 3 shows the angular dependence of these three components with the incident angle of 60 deg reported by Minton et al. For the AO concentrator for material degradation studies, translational energy of impinging AO should be conserved after the reflection. Therefore, the effective surface mass in this study was chosen to maximize the flux of high-energy component. From Fig. 3, it is obvious that the high-energy IS component shows the peak at the exit angle of 64 deg, not the specular direction of 60 deg. Figure 4 shows the computer-simulated results of the average exit angle of the scattered F atom that collides with the target surface with incident angle of 60 deg as a function of effective surface mass. It was calculated that the average exit angle of 64 deg is obtainable with the effective surface mass of 200 amu. In the Hard-Cube model, the effective mass is a parameter which represents the difference in actual scattering process including inelastic scattering. The greater effective mass basically means that the process is closer to the elastic scattering. The effective mass of 200 suggests that the scattering of AO at Pyrex is rather elastic. This is probably related to the fact hat Pyrex is a material with a very small recombination cross-section of AO (inert to AO). Thus, effective surface mass was settled in 200 amu in the following calculation, $\mu = 0.08$. Figure 5 shows the difference between incident and exit angles of AO reflected at the solid surface as a function of incident angle. The difference between incident and exit angles depends on its incident angle. The largest difference in exit and incident angles was calculated to be 5 deg at the incident angle of 42 deg. The computational results shown in Fig. 5 were used to calculate the exit angle of scattered AO in the trajectory calculations. Note that only the average scattering

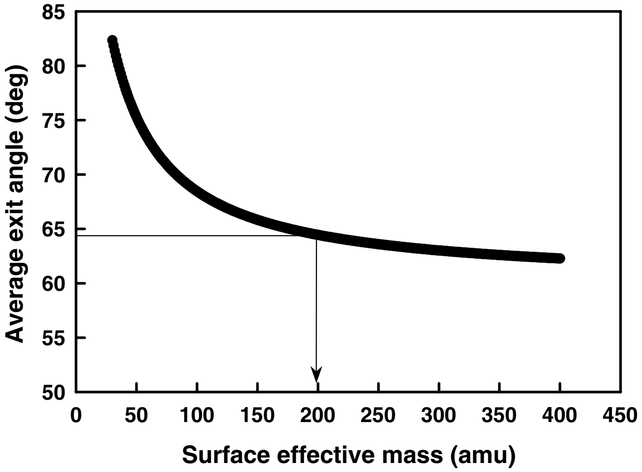

Fig. 4 Computational results of the average exit angles of AO reflected at the solid surface as a function of surface effective mass.

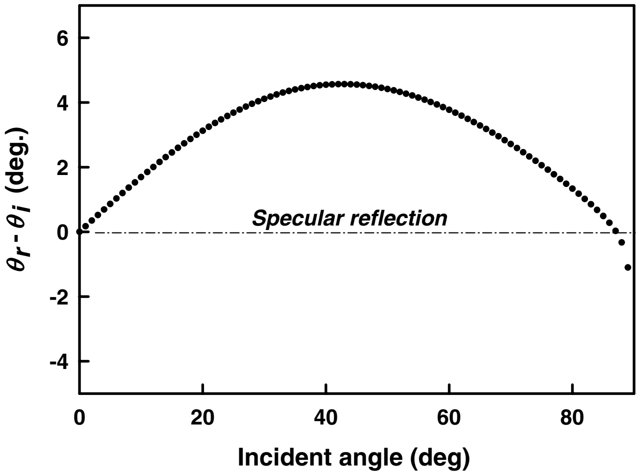

Fig. 5 Computational results of the difference in the incident and exit angles of 5 eV AO as a function of the incident angle.

angle was calculated in this simulation and quantitative analysis cannot be achieved theoretically.

IV. Experimental Details

A. Atomic Oxygen Beam Source

The AO beam source used in this study was a laser detonation AO source. This type of AO source was originally developed by Physical Sciences Incorporation (PSI) [7]. It uses laser-induced breakdown phenomenon of oxygen gas. Principle of operation in the AO source is described as follows. Pure oxygen gas is introduced into the nozzle throat through a pulsed supersonic valve. A giant laser pulse of carbon dioxide laser is focused to oxygen gas at the nozzle throat. By absorbing laser energy, high-density and high-temperature oxygen plasma is formed at the nozzle throat. Once plasma is formed, the plasma propagates with absorbing the laser energy that is included in the tail of the laser pulse. The plasma propagation is along with the incident laser axis and oxygen molecules are decomposed and accelerated at the shockfront of the plasma propagation. Thus, an intense hyperthermal AO beam pulse is formed. The laser detonation AO source is attached to the space environment simulation facility at Kobe University. The AO beam is always monitored by the time-of-flight (TOF) measurement system consisting in a quadrupole mass spectrometer (QMS) and a multichannel scalar.

The flux of a 5 eV AO beam was measured by an Ag-coated quartz crystal microbalance (QCM) with an accommodation coefficient of 0.62 [3]. The principle of measurement is explained in following section. Typical AO fluxes used in the following experiments were in the range of 10^{14} atoms/cm^2/s.

B. Detection of Reflected Atomic Oxygen by Ag-QCM

A flux of AO reflected at the reflector surface was also measured using QCM with silver electrodes [8]. The resonant frequency of a QCM decreases with time when AO oxidizes silver electrodes of QCM. Since silver is not oxidized by O_2 but by AO at room temperature, formation of silver oxide signifies atomic oxygen reaction at the silver surface. A change in mass of the silver film was recorded by measuring the resonance frequency of QCM with a resolution of 0.1 Hz during atomic oxygen exposure. Frequency shift of QCM is expressed in the formula

$$\Delta f = -f_0^2 \Delta W / NA\rho \tag{2}$$

where N is the frequency constant, A is the electrode area, ρ is the density of quartz, and f_0 is the resonant frequency. Because N, A, ρ, and f_0 are known factors, one can calculate the mass change ΔW of the sensor crystal from the frequency shift Δf of the QCM. It is natural to consider that reaction yield of materials with AO depends on its translational energy. Evidently, reaction yield of polyimide depends strongly on the translational energy of AO. It has been reported that the polyimide erosion by 1.1 eV AO is much lower than that by 5.0 eV beam [9]. The translational energy of the reflected AO may be decreased due to inelastic scattering and the reaction yield of silver would also be affected. Since the effect of translational energy on silver oxidation is unknown, the reaction yield of AO with silver surface was assumed to be 1.0, instead of 0.62 for the 5 eV case. Therefore, the calculated flux in this study was the lower bound of the actual AO flux reflected (the concentration efficiency could be underestimated).

V. Results and Discussion

A. Material of the Reflector

Reflection of atoms/molecules at solid surfaces has been investigated as gas-surface scattering phenomena. It has been recognized that AO would react with solid surfaces and form oxide, recombine to molecular oxygen, or simply scatter when it scattered at solid surfaces. Therefore, the material of the reflector surface, which gave small cross-section of recombination of AO, should be selected. Table 2 lists the recombination cross-section of AO at various solid surfaces [10]. It is obvious that Pyrex gives the lowest recombination cross-section of AO. In contrast, Au is known to be an AO-resistant metal but has relatively large recombination cross-section. Thus, these two materials were chosen as candidates for reflecting mirror surfaces of AO concentrator and experimentally tested.

Pyrex and Au surfaces tested were optical mirrors with 7.62 cm in diameter. These reflecting surfaces were placed at 46.5 cm downstream from the nozzle. Incident and exit angles of AO were settled at 45 deg. Flux of AO reflected was measured by the Ag-QCM detector located 10.0 cm from the reflector surface. Figure 6 indicates the mass gain of QCM during the test. AO fluxes reflected by Au and Pyrex surfaces were measured from the slope of the graph. It was calculated that the AO fluxes reflected by Au and Pyrex surfaces were 1.13×10^{14} and 1.48×10^{14} atoms/cm^2/s, respectively. In contrast,

Table 2 Recombination cross-section of AO at solid surfaces [10]

Metals		Oxides	
Material	Recombination cross-section	Material	Recombination cross-section
Ag	2.4×10^{-1}	CuO	4.3×10^{-2}
Cu	1.7×10^{-1}	Mn_2O_3	1.3×10^{-2}
Fe	3.6×10^{-2}	Fe_2O_3	5.2×10^{-3}
Ni	2.8×10^{-2}	CrO_3	2.5×10^{-4}
Au	5.2×10^{-3}	ZnO	4.4×10^{-4}
Mg	2.6×10^{-3}	Pyrex	$3.1–4.5 \times 10^{-5}$

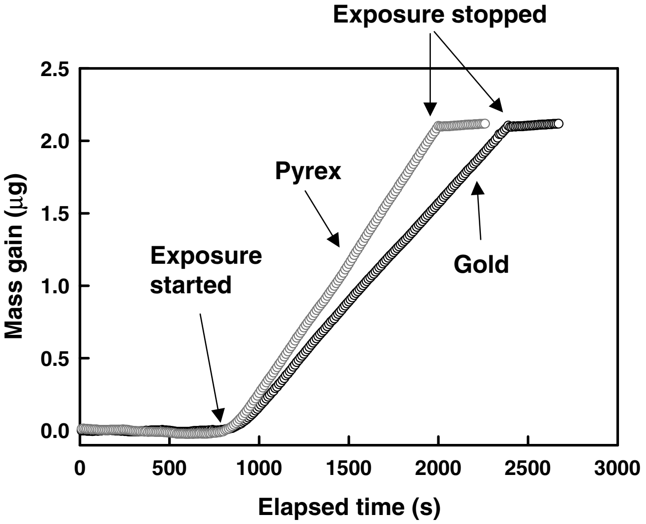

Fig. 6 Mass gain of the Ag-QCM due to oxidation by the AO reflected by two flat reflectors: Au and Pyrex.

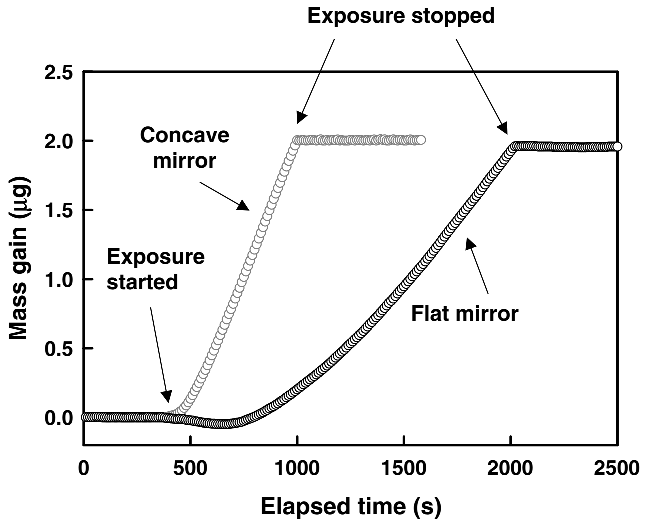

Fig. 7 Mass gain of the Ag-QCM due to oxidation by the AO reflected by two Pyrex reflectors: flat and concave.

AO flux at 56.5 cm away from the nozzle without the reflecting mirror was measured to be 1.7×10^{14} atoms/cm^2/s. By comparing these values, the efficiency of reflection at Au and Pyrex surfaces was evaluated to be 66.5 and 87.1%, respectively. It was identified from these results that the recombination cross-section of the reflector surface is important to maximize the efficiency of AO concentration.

B. Shape of the Reflector

A reflecting surface, which has curvature, may indicate higher efficiency of concentration. To evaluate this effect, two Pyrex reflectors were prepared: flat and concave mirrors. The concave mirror used in this experiment was 15.24 cm in the radius of curvature of the reflecting surface (7.62 cm in focal length). Configuration of the experiment was the same as that described in a preceding section; incident angle of 45 deg, exit angle of 45 deg, and distance between the mirror surface and the Ag-QCM detector was 7.0 cm. Figure 7 indicates the frequency shift of the Ag-QCM during AO exposure. AO flux reflected by the concave reflector was 3.18×10^{14} atoms/cm^2/s, which is twice as large as that reflected by the flat reflector 1.60×10^{14} atoms/cm^2/s. It was thus concluded that the use of a concave reflector is effective to concentrate AO.

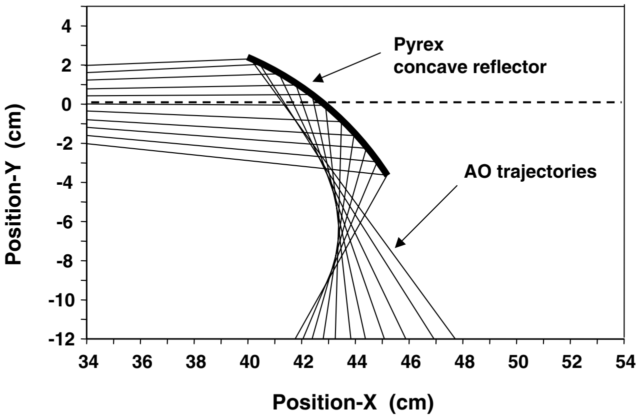

Fig. 8 Computational results of the trajectories of 5 eV AO reflected at the Pyrex concave reflector.

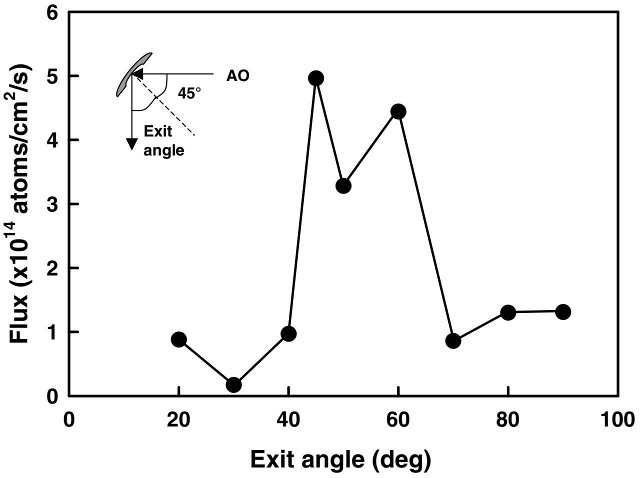

Fig. 9 Experimental results on the angular dependence of AO flux reflected at the Pyrex concave reflector.

C. Verification of the Computational Results

The experiment described in the preceding section was carried out without calculating actual focal point with the Hard-Cube model. The AO flux measured may not be the maximum value at the actual focal point. Thus, the focal point of AO reflected at the Pyrex reflector in the experimental configuration was computer-simulated. The trajectories of AO reflected at the Pyrex concave reflector are shown in Fig. 8. It is observed that AO is focused near the position $x = 44$ cm, $y = -6$ cm even though aberration is fairly large. This focal position corresponds to the average exit angle of 55 deg (incident angle is 45 deg). This result indicates that AO was concentrated at the exit angle 10 deg wider than the specular direction. It was thus predicted that the AO flux measured in the previous section was not the maximum flux concentrated. The computational result was compared with those measured in an actual experiment in the same configuration. Flux measurement of the focused AO was carried out with the exit angle between 20–90 deg by rotating the Ag-QCM detector. Detection of AO was made by Ag-QCM with the mirror-detector distance of 8.0 cm. The results are shown in Fig. 9. As is clearly seen in Fig. 9, the AO flux reflected shows its peak at the exit angle between 45 and 60 deg. The Hard-Cube model used in this study is known as a simple scattering model, however, it is confirmed that the Hard-Cube model successfully predicts the reflecting direction of AO with the concave reflector.

D. Effect of Multiple Reflectors

Three concave reflectors were used to demonstrate the capability for increasing AO flux. The experimental setup is shown in Fig. 10. Incident angle of AO for the upper and the center reflectors

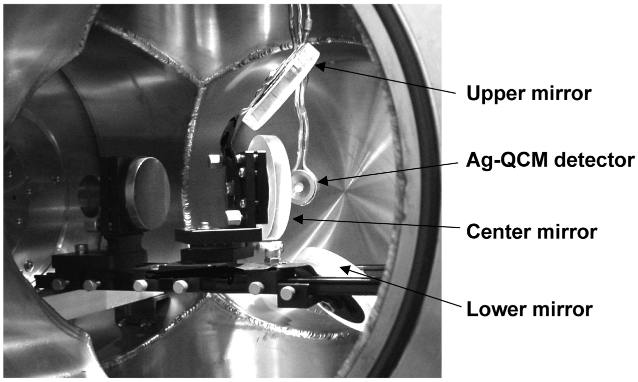

Fig. 10 The experimental configuration of the atomic oxygen concentration with three Pyrex concave reflectors.

Table 3 AO fluxes concentrated by the three Pyrex concave reflectors shown in Fig. 10.

No. of reflectors	Flux measured by Ag-QCM ($\times 10^{14}$ atoms/cm^2/s)
0	1.92
1	0.58–1.39
2	4.31–5.27
3	13.1

was 45 deg, whereas that for the lower reflector was 55 deg. These reflectors were installed to point their exit directions toward the Ag-QCM detector. The AO flux detected by the Ag-QCM in this experimental setting is listed in Table 3. AO flux concentrated with a single reflector is distributed between 0.58 and 1.39×10^{14} atoms/cm^2/s depending on their mirror-QCM distances (direct flux without mirror at the same distance from nozzle was 1.92×10^{14} atoms/cm^2/s). With three reflectors, the AO flux reaches as high as 1.31×10^{15} atoms/cm^2/s, which is more than six times greater than the original flux. Note that the AO flux detected without reflector was subtracted as background, thus, the preceding fluxes mentioned are the net AO fluxes reflected by the reflectors. From the experiment demonstrated here, the capability for increase AO flux by the reflector system was successfully demonstrated.

VI. Conclusions

Use of Pyrex reflectors to increase AO flux in LEO was proposed in this study. The reflection efficiency of 5 eV AO at Pyrex surface was measured to be as high as 87.1%. The focal point of AO reflected was successfully predicted by the simple computer simulation based on the Hard-Cube model. The computational results on the trajectories of AO reflected at the Pyrex concave mirror were compared to experimental results, and good correlation was obtained. It was demonstrated that the AO flux at the focal point increased one order of magnitude higher than the initial exposure condition with three Pyrex reflectors. Even though the directionality and energy distribution of the incoming AO may be partially lost by the reflection, the AO concentrator would allow us to see early previews of AO effects that would not be seen with low fluence AO exposures.

Acknowledgments

A part of this work was supported by the grant-in-aid of scientific research from the Japan Society for the Promotion of Science, and the Space Utilization Promotion from the Japan Space Forum.

References

[1] Applin, J. I., Conell, J. W., Dillman, R. A., Harvey, G. A., Humes, D. H., Jones, J. L., Kinard, W. H., Thibeault, S. A., Kiefer, R. L., Orwoll, R. A., Harrison, J. E., Ronesi, V. M., and Pippin, G. A., Final Report, United States Developed ESEM Experiments: Evaluation of Space Environment and Effects on Materials, available at the website http://setas-www.larc.nasa.gov/esem/esem_final_report.html.

[2] Yokota, K., Seikyu, S., Tagawa, M., and Ohmae, N., "A Quantitative Study in Synergistic Effects of Atomic Oxygen and Ultraviolet Regarding Polymer Erosion in LEO Space Environment," *Proceedings of the 9th International Symposium on Materials in a Space*, SP-540, ESA, Noordwijk, The Netherlands, 16–20 June, 2003, pp. 265–272.

[3] Tagawa, M., Yokota, K., Kinoshita, H., and Ohmae, N., "Application of Quartz Crystal Microbalance for Polymer Degradation Studies Regarding Atomic Oxygen Activities in Low Earth Orbit," *Proceedings of the 9th International Symposium on Materials in a Space*, SP-540, ESA, Noordwijk, The Netherlands, 2003, pp. 247–252.

[4] Kinoshita, H., Tagawa, M., Yokota, K., and Ohmae, N., "Nonlinear Phenomenon in the Mass Loss of Polyimide Films Under Hyperthermal Atomic Oxygen Beam Exposures," *High Performance Polymers*, Vol. 13, No. 4, 2001, pp. 225–234.

[5] Logan, R. M., and Stickney, R. E., "Simple Classical Model for the Scattering of Gas Atoms from a Solid Surface," *Journal of Chemical Physics*, Vol. 44, 1966, pp. 195–201.

[6] Minton, T. K., Giapis, K. P., and Moore, T. A., "Inelastic Scattering Dynamics of Hyperthermal Fluorine Atoms on a Fluorinated Silicon Surface," *Journal of Physical Chemistry A*, Vol. 101, 1997, pp. 6549–6555.

[7] Caledonia, G. E., Krech, R. H., Upschulte, B. L., Sonnenfroh, D. M., Oakes, D., and Holtzclaw, K. W., "Fast Oxygen Atom Facility for Studies Related to Low Earth Orbit Activity," AIAA Paper 92-3974, Sept. 1992.

[8] Matijasevic, V., Garwin, E. L., and Hammond, R. H., "Atomic Oxygen Detection by Silver-Coated Quartz Deposition Monitor," *Review of Scientific Instruments*, Vol. 61, 1990, pp. 1747–1749.

[9] Yokota, K., Tagawa, M., and Ohmae, N., "Temperature Dependence in Erosion Rates of Polyimide under Hyperthermal Atomic Oxygen Exposures," *Journal of Spacecraft and Rockets*, Vol. 40, No. 1, 2003, pp. 143–144.

[10] Greaves, J. C., and Linnet, J. W., "The Recombination of Oxygen Atoms at Surfaces," *Transactions of the Faraday Society*, Vol. 55, 1959, pp. 1323–1330.

D. Edwards
Associate Editor